PROCEEDINGS OF SCIENCE

SUSY searches in ATLAS and CMS

Arka Santra* **on behalf of the ATLAS and CMS collaborations**
Instituto de Fisica Corpuscular, CSIC and Universidad de Valencia, Parque Cientifico, C/Catedratico Jose Beltran, 2, 46980, Paterna, Espana.
E-mail: santra.arka@ific.uv.es

Supersymmetry is one of the most popular beyond-standard-model theories at present. Searches for supersymmetry is one of the main goals of the multipurpose experiments like ATLAS and CMS at the LHC. Both experiments have conducted numerous searches for supersymmetry with a wide variety of final states to date. In this paper, a few of the searches will be discussed from both experiments. The datasets discussed here were gathered during the *pp* collisions with center of mass energy of 13 TeV. As no signs of supersymmetric particles were found, the limits on different supersymmetry scenarios were set.

Corfu Summer Institute 2018 "School and Workshops on Elementary Particle Physics and Gravity" (CORFU2018)
31 August - 28 September, 2018
Corfu, Greece

*Speaker.

PoS(CORFU2018)070

1. Introduction

The Standard Model (SM) of particle physics is one of the most successful theories at present. But there are many questions which are unanswered by it, for example, the hierarchy problem or the presence of dark matter. Supersymmetry (SUSY) [1 – 6] is one of the most popular and well motivated beyond standard model theories. This theory postulates a fundamental symmetry of spacetime that relates all the SM particles to partners having their spins shifted by 1/2.

In general, SUSY provides elegant solutions to some of the problems unanswered by the SM. The radiative corrections to the Higgs boson mass become very large when a fermion couples with the Higgs field. But the radiative corrections from bosonic particles are of opposite sign compared to those from fermionic particles and hence can cancel out the contribution of fermions. SUSY naturally imposes this relation and stabilizes the Higgs boson mass at a value compatible with the measured value of 125 GeV [7]. In SUSY scenarios, a new quantum number named R-parity [8] is introduced and the assumption that it is a conserved quantity leads to the prediction that SUSY particles are produced in pairs. In addition R-parity conserving SUSY theories require that the lightest supersymmetric particle (LSP) is stable and electrically neutral, thus making it an excellent candidate for the dark matter.

Searching for SUSY is one of the main goals of the multipurpose detectors ATLAS and CMS at the LHC. Numerous searches have been conducted by these experiments with a wide variety of final states connected to a number of different SUSY models. The datasets discussed in this proceedings were gathered during the pp collisions at the center of mass energy of 13 TeV in 2015-2017. The integrated luminosity of these datasets vary from 36 fb^{-1} (2015-2016 period) to 80 fb^{-1} (2015-2017 period).

A typical SUSY search uses a set of selection criteria applied to various observables to select different particles like photons, electrons, muons and hadronic jets. Control Regions (CR) are defined by other selection criteria with the aim of providing a sample of events dominated by a certain SM background and having minimal signal contamination. The CR is used to estimate the number of background events in the signal region (SR) which are designed to have optimum signal-to-background ratio. The reliability of the background estimate in the SR is validated in the validation region (VR). The VR is designed to be similar to the SR. A typical SUSY search diagram is represented in Fig. 1.

2. Search for strongly produced SUSY

The production of squarks ($\tilde{q}$) and gluinos ($\tilde{g}$), the so-called strong production, has the highest production cross-section at the LHC. Therefore it is still one of the benchmarks of the SUSY search at the LHC. Since the production cross-section is much higher than the electroweak production, this kind of production is relatively easy to search for compared to the electroweak production. In general, the search can be done by targeting a final state with high transverse momentum (p_{T}) particles (hadronic jets, possible leptons, etc) and missing transverse energy ($E_{\mathrm{T}}^{\mathrm{miss}}$). There are two main approaches followed to search for strong production in the ATLAS experiment. One is the conventional method, where a typical discriminating variable, such as effective mass (m_{eff}, scalar sum of p_{T} of all jets, possible leptons and $E_{\mathrm{T}}^{\mathrm{miss}}$) or $E_{\mathrm{T}}^{\mathrm{miss}}$ is chosen and then its distribution

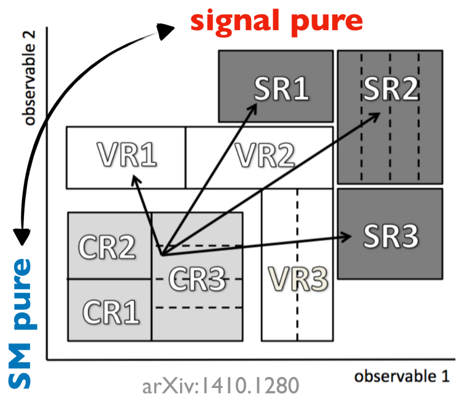

Figure 1: A simplified diagram showing the interplay of control region (CR), validation region (VR) and signal region (SR) [9].

is estimated in the SR. The regions with high values of this variable are expected to be more populated, than others, in SUSY events compared to SM. The other approach is to create Recursive Jigsaw Reconstruction (RJR) variables [10, 11]. These kinematic variables are defined on an event-by-event basis. These variables show very good sensitivity for searches with compressed SUSY mass spectrum.

2.1 R-Parity conserving searches

R-parity conserving (RPC) SUSY theories are at the forefront of the SUSY searches at the ATLAS and CMS experiments. In this theories, the final state always contains an LSP which escapes detection. Hence, the missing energy plays an important role for the search of this kind of models.

2.1.1 Multi-b search

Pair produced gluinos may decay via top or bottom squarks in events with multiple jets originating from the hadronization of b-quarks (popularly known as b-jets), high $E_{\mathrm{T}}^{\mathrm{miss}}$ and potentially additional light quarks jets or/and isolated charged lepton. There was a dedicated search in the ATLAS experiment for this type of gluino decays generally known as multi-b search [12, 13] as the final state contains b-jets. The simplified decay topologies Gbb and Gtt are sketched in Fig. 2.

For this analysis, a number of signal regions were constructed depending on the number of b-jets in the final state, light quark jets, $E_{\mathrm{T}}^{\mathrm{miss}}$, high m_{eff} and number of leptons (0 or 1). A powerful variable to discriminate signal from the background is the total jet mass defined as:

$$M_J^{\Sigma} = \sum_{i \leq 4} m_{J,i} \tag{2.1}$$

where $m_{J,i}$ is the mass of the large radius (Radius parameter R=1.0) re-clustered jet i in the event. The distribution of this variable for the 0-lepton state is shown in Fig. 3. Other discriminating variables like $E_{\mathrm{T}}^{\mathrm{miss}}$ and m_{eff} are shown in Fig. 4.

No excess was found in any of the signal regions and hence exclusion limits were put on the considered model. The mass limit on gluino is extended to 2.1 TeV (Fig. 5).

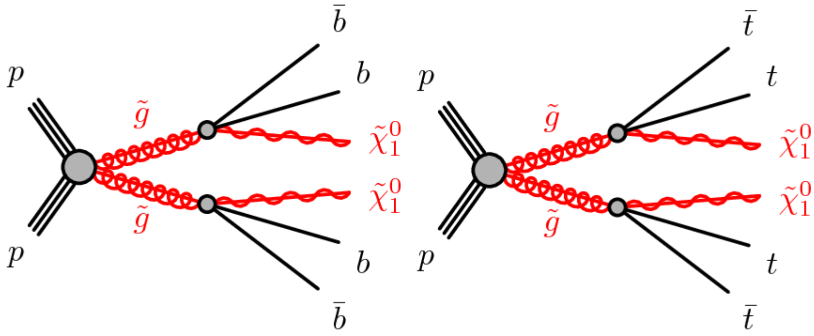

Figure 2: The decay topologies targeted in the Gbb (left) and Gtt (right) models [13].

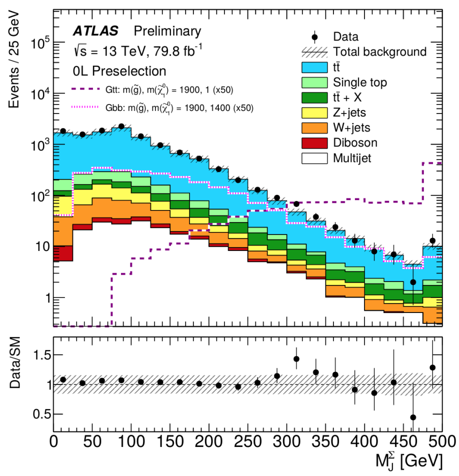

Figure 3: Total jet mass variable M_J^Σ for the 0 lepton preselection region. Reprinted from the ATLAS analysis Ref. [13].

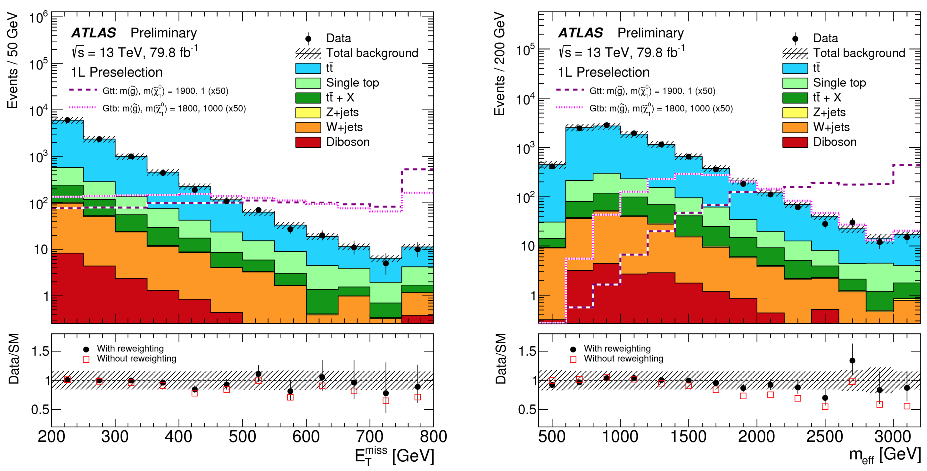

Figure 4: $E_{\mathrm{T}}^{\mathrm{miss}}$ and m_{eff} distributions for 1 lepton preselection region (from the ATLAS analysis [13]).

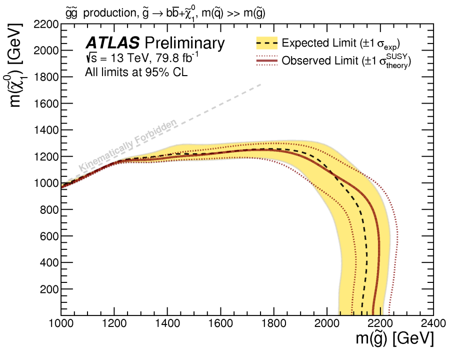

Figure 5: The ATLAS exclusion limit in the neutralino ($\tilde{\chi}_1^0$) and gluino ($\tilde{g}$) mass plane for the Gbb model [13].

2.1.2 GMSB search with one photon and one lepton

SUSY models with general gauge-mediated (GGM) supersymmetry breaking (GMSB) and the additional assumption that R-parity is conserved often lead to final states with photons and $E_{\mathrm{T}}^{\mathrm{miss}}$. In GGM models, the LSP is gravitino ($\tilde{G}$) which is stable and weakly interacting. The gravitino, if produced at the collisions, leave the detector without being detected, giving rise to $E_{\mathrm{T}}^{\mathrm{miss}}$. Additionally, final state may contain a lepton which offers a unique opportunity to probe the branching fractions of SUSY particles. This makes photon plus lepton in addition with $E_{\mathrm{T}}^{\mathrm{miss}}$ an important part of the SUSY search program at the LHC. The decay topologies of this kind of models are shown in Fig. 6. The CMS experiment has searched for this signature in pp collision with $\sqrt{s} = 13$ TeV data with integrated luminosity of 35.9 fb^{-1} [14].

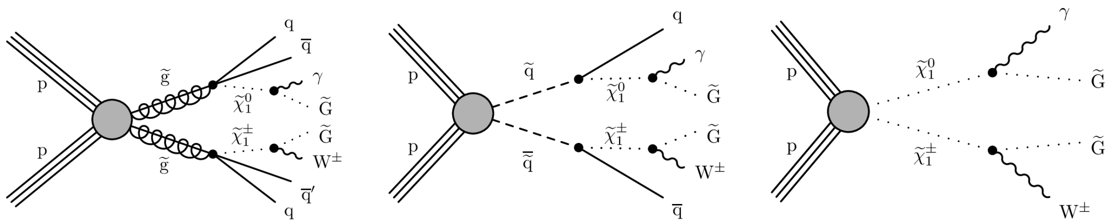

Figure 6: Different decay topologies showing photon and leptons in the final state: T5Wg (left) model where gluino decays to $\tilde{\chi}_1^0$, T6Wg (center) model where squarks decay to $\tilde{\chi}_1^0$ and TChiWg (right) model where $\tilde{\chi}_1^0$ decays to photon and gravitino ($\tilde{G}$) [14].

In this analysis, the data are examined in the bins of the transverse energy of photon, magnitude of missing transverse momentum ($E_{\mathrm{T}}^{\mathrm{miss}}$ or $p_{\mathrm{T}}^{\mathrm{miss}}$) and scalar sum of jet energies (H_{T}). The signal regions require high $E_{\mathrm{T}}^{\mathrm{miss}}$ ($E_{\mathrm{T}}^{\mathrm{miss}} > 120$ GeV). For this analysis, three types of background were encountered. First one is without prompt photon, where photon originates from the pile up. This background is estimated by finding the rate of photon mis-identification in data. The second type of background involves events without prompt lepton. The leptons come from mis-identified jets and hadronization of heavy flavor quarks. This type of background is also estimated from data. The third type, the electroweak background (consisting of $WW\gamma$, $WZ\gamma$ and $t\bar{t}\gamma$) is evaluated using simulated samples. The E_T^{miss} distributions for electron-photon and muon-photon channels are shown in Fig. 7.

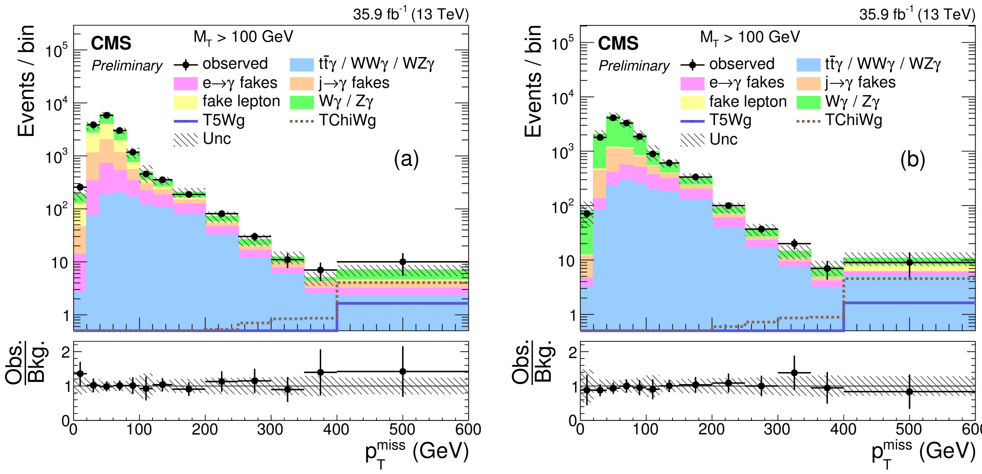

Figure 7: Missing transverse energy (E_T^{miss} or p_T^{miss}) distributions for electron-photon (left) and muon-photon (right) channels. Taken from the CMS Analysis [14].

Since there is no excess in data in the signal region with respect to the SM background, this analysis put exclusion limits on the production cross-sections as a function of SUSY particle mass (Fig. 8).

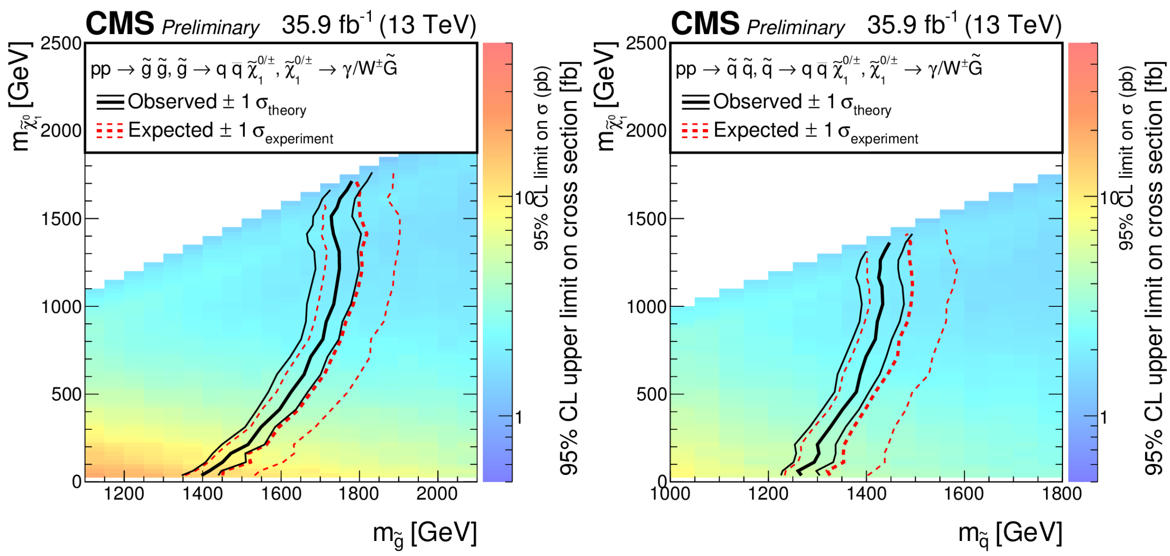

(a) (b)

Figure 8: The observed and expected 95% CL exclusion contours for gluino/squark mass ($m_{\tilde{g}/\tilde{q}}$) versus neutralino mass ($m_{\tilde{\chi}_1^0}$) and the 95% upper limits for the pair production cross-sections. On the left, T5Wg model has been used and on the right, T6Wg model has been used. A 50% branching fraction for $\tilde{g}(\tilde{q}) \rightarrow \tilde{\chi}^0/\tilde{\chi}^{\pm}q\bar{q}$ is assumed [14].

2.1.3 Status of contraints on RPC scenarios

In simplified model approach, the mass limits for the generic RPC searches are the following:

- $M_{\tilde{g}} \lesssim \mathscr{O}(1 \text{ TeV}) - \mathscr{O}(2 \text{ TeV})$ @95% CL
- $M_{\tilde{q}} \lesssim \mathscr{O}(0.5 \text{ TeV}) - \mathscr{O}(1.5 \text{ TeV})$ @95% CL
- $M_{\tilde{t}} \lesssim \mathscr{O}(0.7 \text{ TeV}) - \mathscr{O}(1.1 \text{ TeV})$ @95% CL

A summary of mass limits from the ATLAS and CMS experiments for the RPC searches can be found in Fig. 9. It should be worth noting that these limits are highly model-dependent and they mostly pertain to simplified topologies, where 100% branching ratios are assumed.

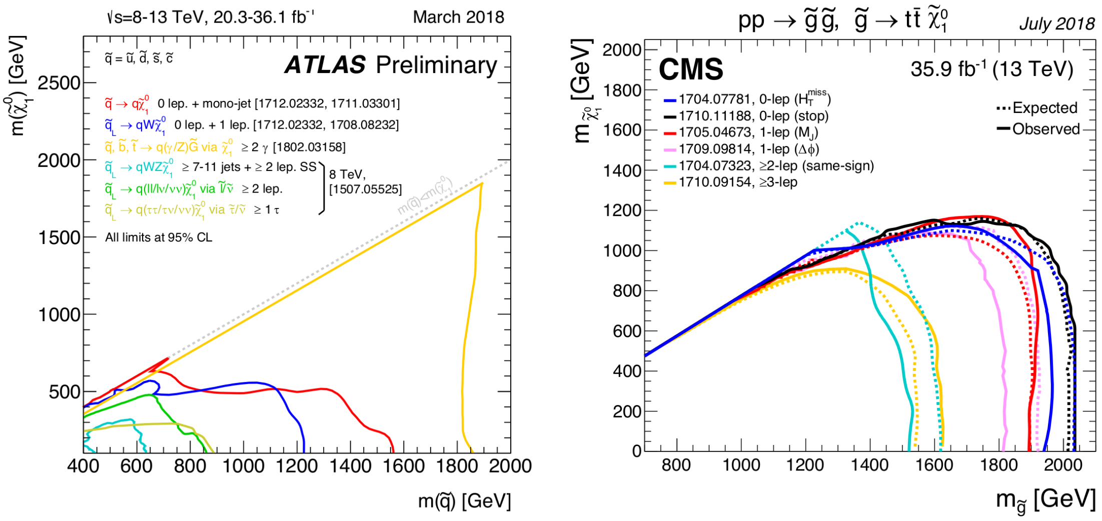

Figure 9: A summary of mass limits for RPC searches presented by the ATLAS (left) [15] and CMS (right) [16] experiments.

2.2 R-Parity violating searches

In addition to R-parity conserving models where the LSP is stable, the ATLAS and CMS experiments have both studied R-parity violating (RPV) scenarios, where the LSP is not stable and decays to SM particles. In this kind of models, where RPV terms are present in the SUSY superpotential, either lepton or baryon number violation is allowed. This brings to a number of final states not considered in the RPC searches.

2.2.1 Search for pair-produced three-jet resonances

Multijet final states at hadron colliders are a signature of many SUSY models, even though this kind of final states heavily suffer from large SM backgrounds. There is a CMS analysis which search for pair-produced resonances, each decaying to three quarks giving rise to multijet events in pp collisions [17]. The decay topology can be found in Fig. 10. In this analysis, events with at least six high-p_T jets were selected to search for evidence of three-jet resonances.

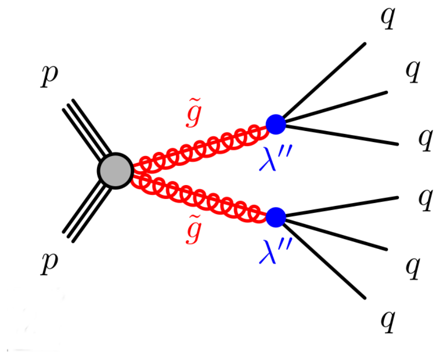

Figure 10: Feynman diagram showing an RPV scenario where six hadronic jets are produced in the final state [17].

Dalitz plots, a very useful technique to study three-body decays [18], were used to study the internal dynamics of the three-body systems and discriminate between signal containing gluino decays and background consisting of QCD multijets. Here, the invariant mass of three dijet pairs (inside a triplet) was constructed: m_{12}, m_{23} and m_{13}. Normalizing these dijet invariant masses, a Dalitz variable for a triplet was constructed:

$$\hat{m}(3,2)^2_{i,j} = \frac{m^2_{ij}}{m^2_{ijk} + m^2_i + m^2_j + m^2_k} \tag{2.2}$$

where $i, j, k \in \{1,2,3\}$ and m_i is the individual-jet mass and m_{ijk} is the mass of the triplet. Pair masses within the triplet as described in Eq. (2.2) are shown in Fig. 11. This figure shows that while the background QCD events populate the edge, the signal events fill up the center. Keeping this in mind, a variable named mass distance squared (MDS) is constructed, as follows:

$$MDS[3,2] = \sum_{i>j} (\hat{m}_{ij} - \sqrt{1/3})^2 \tag{2.3}$$

The distribution of MDS[3,2] variable is plotted in Fig. 12 (left). Since no excess over the background was found in the signal regions, this analysis set the exclusion limit on the production cross-section as a function of the resonance mass shown in Fig. 12, right.

3. Third generation production

A strong motivation for third generation searches is coming from the Higgs mass measurement [7]. The Higgs mass seems to be unnaturally light and the existing squark and gluino exclusion limits reach up to the TeV scale. Naturalness [19, 20] arguments in SUSY models suggest that the mass of the lightest top squark ($\tilde{t}_1$) would be of the same order of the top quark [21, 22]. Top squark may be pair-produced with subsequent decays which are induced by flavor-violating effects into charm quark and an LSP, $\tilde{t}_1 \to c\tilde{\chi}^0_1$ (Fig. 13). There is a SUSY search in the ATLAS experiment [23] targeting the pair production of top and charm squarks where the charm squark eventually decays into charm quark and an LSP.

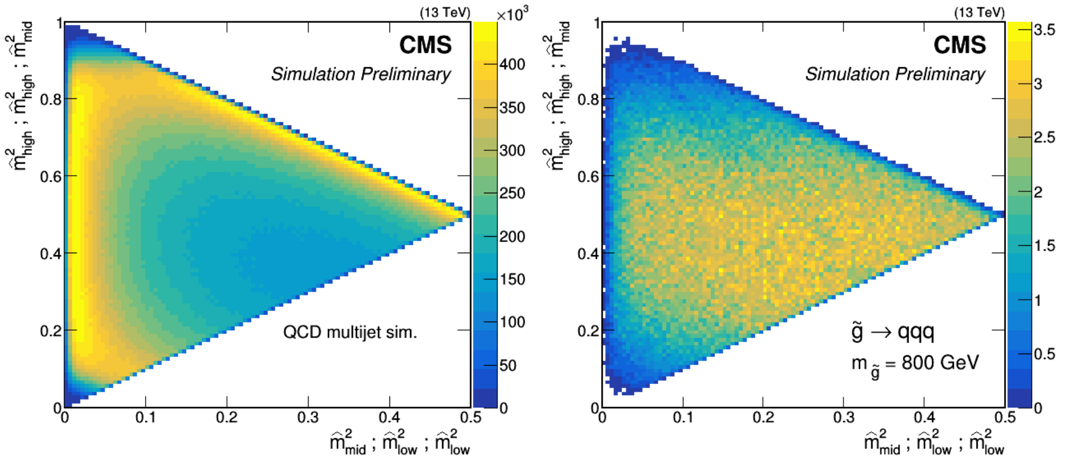

Figure 11: Plot of pair masses within the triplet, as defined in Eq. (2.2). Here QCD triplets (left) cluster at the edge, but the triplets from signal events (right) populate the center [17].

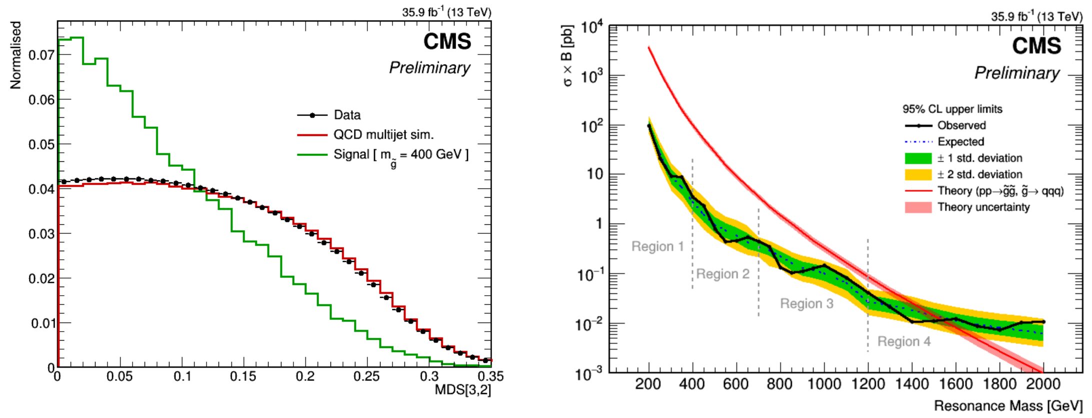

Figure 12: MDS[3,2] variable for signal and QCD triplets (left) and the observed and expected CLs cross-section limits (right). The gray boundaries indicate different mass regions considered in this analysis. Reprinted from the CMS analysis [17].

3.1 SUSY with charm quarks

In this analysis, the signal region requires at least two jets with at least one charm-tagged jet, and high $E_{\mathrm{T}}^{\mathrm{miss}}$. Here the challenging task is to identify charm tagged jets properly. To do that, multivariate discriminants, MV2c100 and MV2c1100 were used to distinguish between charm jets and b-jets and between charm jets and light flavor jets respectively. These discriminants are based on the MV2 algorithm described in Refs. [24, 25]. MV2c100 was trained with b-jets as signal and here background consisted of exclusively charm jets. On the other hand, MV2c1100 was trained with charm jets as signal and background consisted of exclusively light flavor jets. For this analysis, a working point was selected with the charm-tagging efficiency of $\sim 18\%$, a light flavor jet rejection factor of 200, a b-jet rejection factor of 20 and a hadronic τ rejection factor of six. These values were evaluated in a sample of simulated $t\bar{t}$ events. The charm jet tagging rate was measured with a data sample which was rich in $t\bar{t}$ events, where charm jets come from W boson decay. Adequate correction factors were applied to simulated samples in order to match with the tagging rate in data.

This analysis had a significant background from hadronically decaying τ. In order to reduce this background, the transverse mass of the τ, m_{T}^{c} was used. It was found that $m_{\mathrm{T}}^{c} > 120$ GeV could reduce this background to less than 5%.

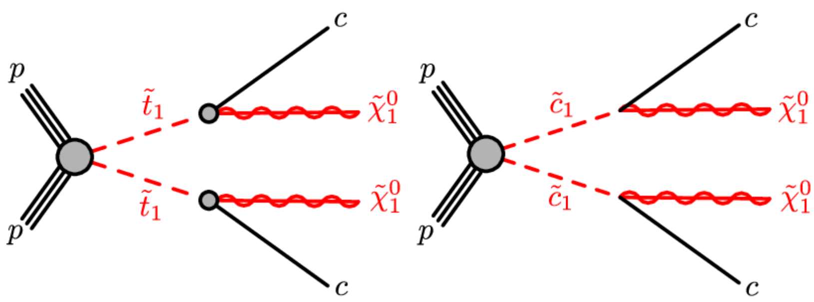

Figure 13: Pair production of top and charm squarks which eventually decay into charm quarks and two LSPs [23].

Depending on the mass difference, there were five different SRs constructed for this analysis. The most significant background for them came from the Z+jets sample ($\sim 50-60\%$ in all SRs). This background was estimated using simulated samples. Other backgrounds like W+jets (where W decays to τ and neutrino), diboson and $t\bar{t}$ were also estimated from the simulated samples. Since no excess over the background was found, the analysis put the exclusion limit on the top/charm squark mass shown in Fig. 14.

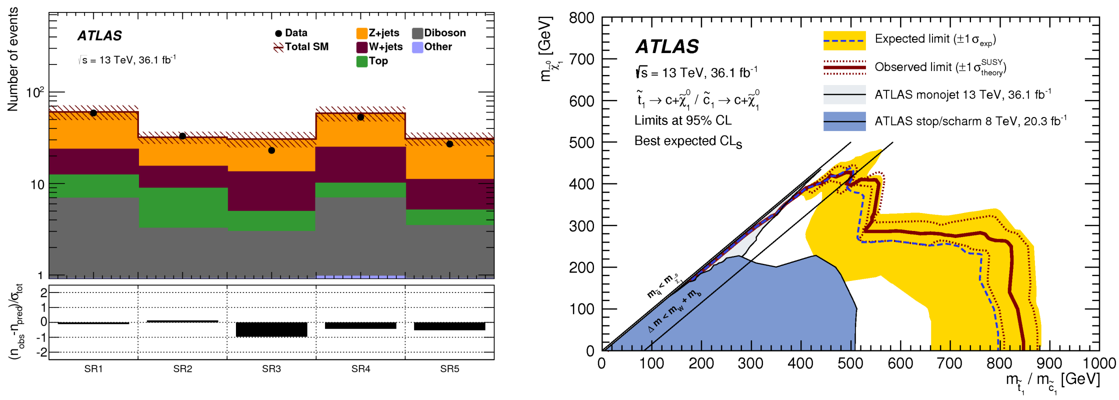

Figure 14: Comparison of data events and the estimated background yields in each of the signal regions (left). Observed and expected exclusion contours at 95% CL in the top/charm squark and neutralino mass plane (right). This is an ATLAS analysis [23].

4. Electroweak searches

If the masses of squarks and gluinos are too large for the LHC collision energy of 13 TeV, they cannot be produced in large numbers at the LHC. In strong-production searches, the mass limits for gluinos and squarks are reaching about 2 TeV. This motivates the search for electroweak production of SUSY particles. Since the cross-section of electroweak production is well below the strong production, there is still a large mass range left to probe.

For electroweak SUSY production, typical searches consider final states with two or three leptons, $E_{\mathrm{T}}^{\mathrm{miss}}$, with or without jets. For most of the searches, most significant background comes from the diboson events. Jet vetoes are generally used to reduce the $t\bar{t}$ events.

4.1 Direct slepton searches

Direct slepton production mechanism is one of the most important electroweak searches at both the CMS [26] and ATLAS [27] experiments. The signal regions require opposite-charge same-flavor dileptons events with a jet veto. A high value of the variable stransverse mass (m_{T2}) [27] was used to suppress WW events. The CMS analysis used $E_{\mathrm{T}}^{\mathrm{miss}}$ bins to search for an excess. The ATLAS analysis used bins of dilepton invariant mass and m_{T2}. Both experiments did not find any significant excess of events and hence they set exclusion limits on the slepton mass (Fig. 15). The CMS experiment put a slepton mass limit at around 450 GeV, whereas the ATLAS experiment set a mass limit at around 520 GeV.

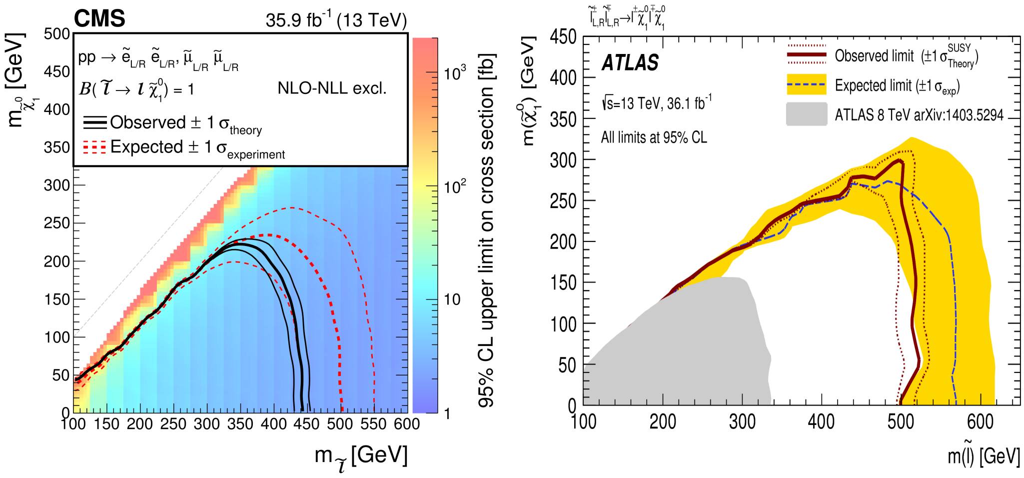

Figure 15: Observed and expected exclusion contour for slepton pair production at the CMS experiment (left) [26] and the ATLAS experiment (right) [27].

4.2 Chargino/neutralino production: 2L/3L+$E_{\mathrm{T}}^{\mathrm{miss}}$ RJR

The electroweakinos ($\tilde{\chi}_1^{\pm}\tilde{\chi}_2^0$) may be pair produced in an electroweak SUSY processes and $\tilde{\chi}_1^{\pm}$ and $\tilde{\chi}_2^0$ decay to a $\tilde{\chi}_1^0$ and a W or a Z boson respectively. The W and Z boson can further decay leading to final states with two or three isolated leptons, which may be accompanied by jets and $E_{\mathrm{T}}^{\mathrm{miss}}$. The Feynman diagrams can be found in Fig. 16. There is an ATLAS analysis [28] searching for this scenario employing recursive jigsaw reconstruction technique in the construction of complementary discriminating variable. Signal regions in this analysis are constructed to probe a wide range of $\tilde{\chi}_1^{\pm}/\tilde{\chi}_2^0$ (assumed to be degenerate) and $\tilde{\chi}_1^0$ masses, having mass differences $\Delta m = m_{\tilde{\chi}_1^{\pm}/\tilde{\chi}_2^0} - m_{\tilde{\chi}_1^0}$ from $\sim$ 100 GeV to $\sim$ 600 GeV.

The RJR technique [10, 11] is a method to recursively construct the decay chain of pair produced heavy particles. Reconstructed view of the event gives rise to a natural basis of kinematic

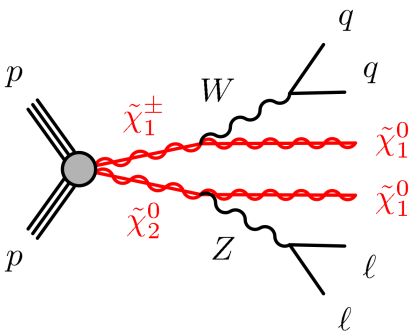

Figure 16: Feynman diagrams of pair production of $\tilde{\chi}_1^{\pm}\tilde{\chi}_2^0$ and their subsequent decays to leptons and $E_{\mathrm{T}}^{\mathrm{miss}}$ through W/Z bosons [28].

observables, calculated by evaluating the momentum and energy of different objects in the event in these reference frames. The background processes are reduced by testing whether the event exhibits the anticipated properties of the decay tree under investigation.

The schematic diagram in Fig. 17 (left) can help understanding this method. Here each event is processed considering the two parent sparticles (labeled 'PP') assigned to two distinct hemispheres $\mathrm{P_a}$ and $\mathrm{P_b}$. Then they decay to particles detected in the detector (visible particle, 'V') and not detected in the detector (invisible particle 'I'). If one considers the 2 lepton + 2 jets final state (Fig. 17, right), one can see that the lepton pair must be associated with the same visible collection and the jet pair must be associated with the other visible collection of the event. So if for an event with 2 leptons and 2 jets, this criteria is not fulfilled, this event is rejected. This way, RJR technique helps to reduce the background events.

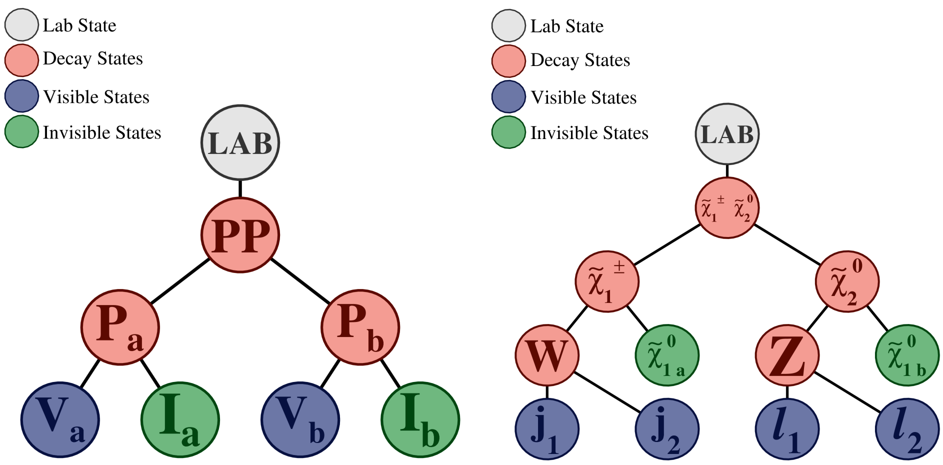

Figure 17: On the left, the standard decay tree of pair produced sparticles. Here parent particle 'P' decays to visible state 'V' and invisible state 'I'. On the right, decay trees for the 2 lepton + 2 jets final state [28].

In most of the signal regions, no excess over the estimated background was found. Only for one region (named ISR) with 3 leptons, a 3σ excess was observed. The conventional analysis with 2 leptons and jets [29] using the same dataset did not find such excess. Observed and expected exclusion limits on the masses of $\tilde{\chi}_1^{\pm}\tilde{\chi}_2^0$ and $\tilde{\chi}_1^0$ are shown in Fig. 18.

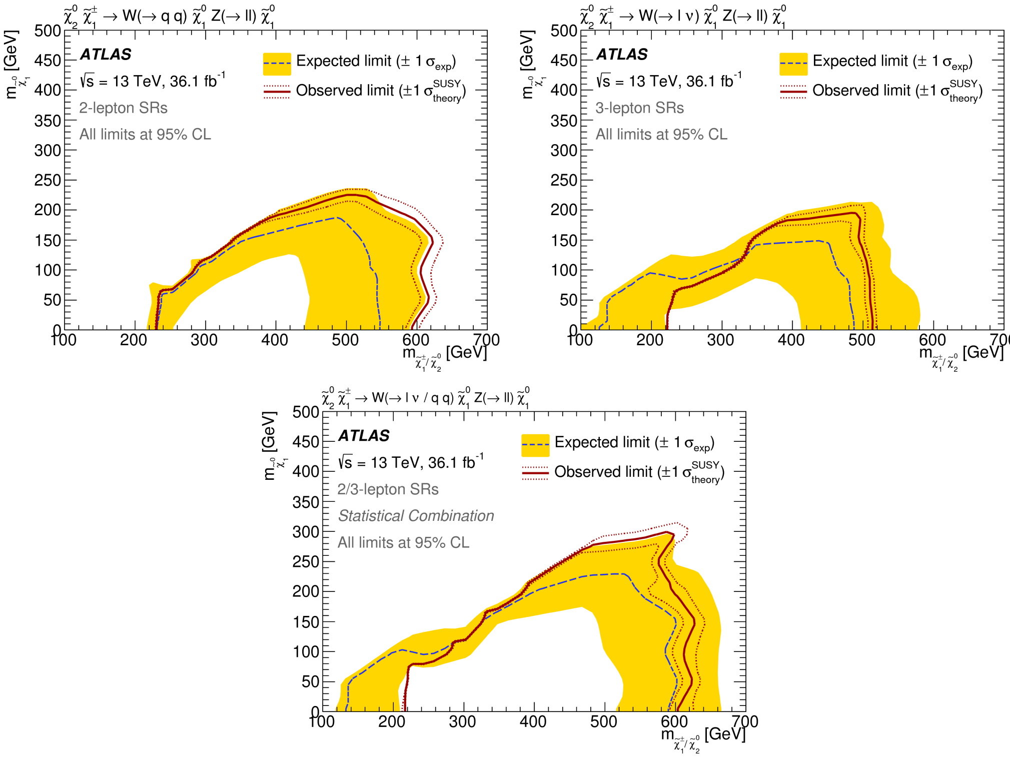

Figure 18: Exclusion limits at 95% CL on the masses of $\tilde{\chi}_1^{\pm}\tilde{\chi}_2^0$ and $\tilde{\chi}_1^0$. The exclusion contour for 2 lepton SRs has been shown on top left, for 3 lepton SRs shown has been shown on top right and the statistical combination of them has been shown on bottom [28].

4.3 Summary of electroweak searches

Many other searches for electroweak SUSY production have been performed by both the ATLAS and CMS experiments that could not be discussed within the scope of these proceedings. Fig. 19 presents the summary exclusion plots from many of the searches as a function of chargino/neutralino masses.

5. Conclusion

Both the ATLAS and CMS experiments are pursuing an extensive search program covering strong and electroweak production of SUSY. A variety of different final states have been considered making use of the data collected so far. A good agreement is found between data and the expected SM background. Both experiments have put limits on the production cross-section of a wide variety of simplified SUSY models. The summary of mass limits published by the ATLAS experiment is shown in Fig. 20. The CMS SUSY searches summary is presented in Fig. 21.

Future searches at the ATLAS and CMS experiments plan to use a significantly higher luminosity (about 140 fb^{-1} for the entire run 2), and a large number of improvements in the analysis software R&D. This will help extending the phase space of sensitivity of a large number of SUSY models as well as looking for uncovered and more difficult regions in the parameter space and testing a large number of new well-motivated physics scenarios.

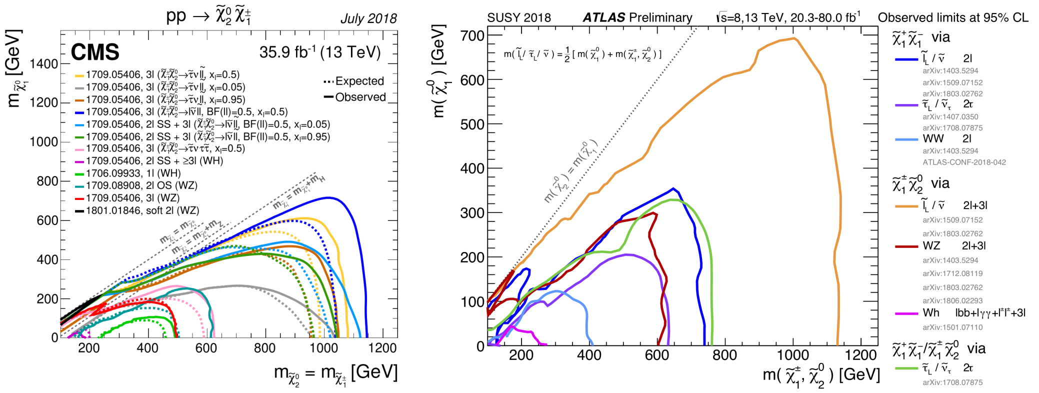

Figure 19: Summary of exclusion contours produced by the CMS (left) [16] and ATLAS (right) [15] experiments for the electroweak SUSY production.

Acknowledgements

The author acknowledges the support by the Severo Ochoa Excellence Centre Project SEV-2014-0398 and the project FPA2015-65652-C4-1-R of the Spanish Ministry of Science, Innovation and Universities (MICIU).

References

[1] Yu. A. Golfand and E. P. Likhtman. Extension of the Algebra of Poincare Group Generators and Violation of p Invariance. JETP Lett., 13:323, 1971. [Pisma Zh. Eksp. Teor. Fiz. 13 (1971) 452]. URL: http://inspirehep.net/record/68412.

[2] D. V. Volkov and V. P. Akulov. Is the Neutrino a Goldstone Particle? Phys. Lett. B, 46:109, 1973. doi:10.1016/0370-2693(73)90490-5.

[3] J. Wess and B. Zumino. Supergauge Transformations in Four-Dimensions. Nucl. Phys. B, 70:39, 1974. doi:10.1016/0550-3213(74)90355-1.

[4] J. Wess and B. Zumino. Supergauge Invariant Extension of Quantum Electrodynamics. Nucl. Phys. B, 78:1, 1974. doi:10.1016/0550-3213(74)90112-6.

[5] S. Ferrara and B. Zumino. Supergauge Invariant Yang-Mills Theories. Nucl. Phys. B, 79:413, 1974. doi:10.1016/0550-3213(74)90559-8.

[6] Abdus Salam and J. A. Strathdee. Supersymmetry and Nonabelian Gauges. Phys. Lett. B, 51:353, 1974. doi:10.1016/0370-2693(74)90226-3.

[7] The ATLAS and CMS Collaborations, "Combined Measurement of the Higgs Boson Mass in pp Collisions at $\sqrt{s} = 7$ and 8 TeV with the ATLAS and CMS Experiments", Phys. Rev. Lett., vol. 114, p. 191803, 2015.

[8] G. R. Farrar and P. Fayet, "Phenomenology of the production, decay, and detection of new hadronic states associated with supersymmetry", Phys. Lett. B, vol. 76, p. 575, 1978.

[9] Baak, M., Besjes, G.J., Cote, D. et al. Eur. Phys. J. C (2015) 75: 153. https://doi.org/10.1140/epjc/s10052-015-3327-7

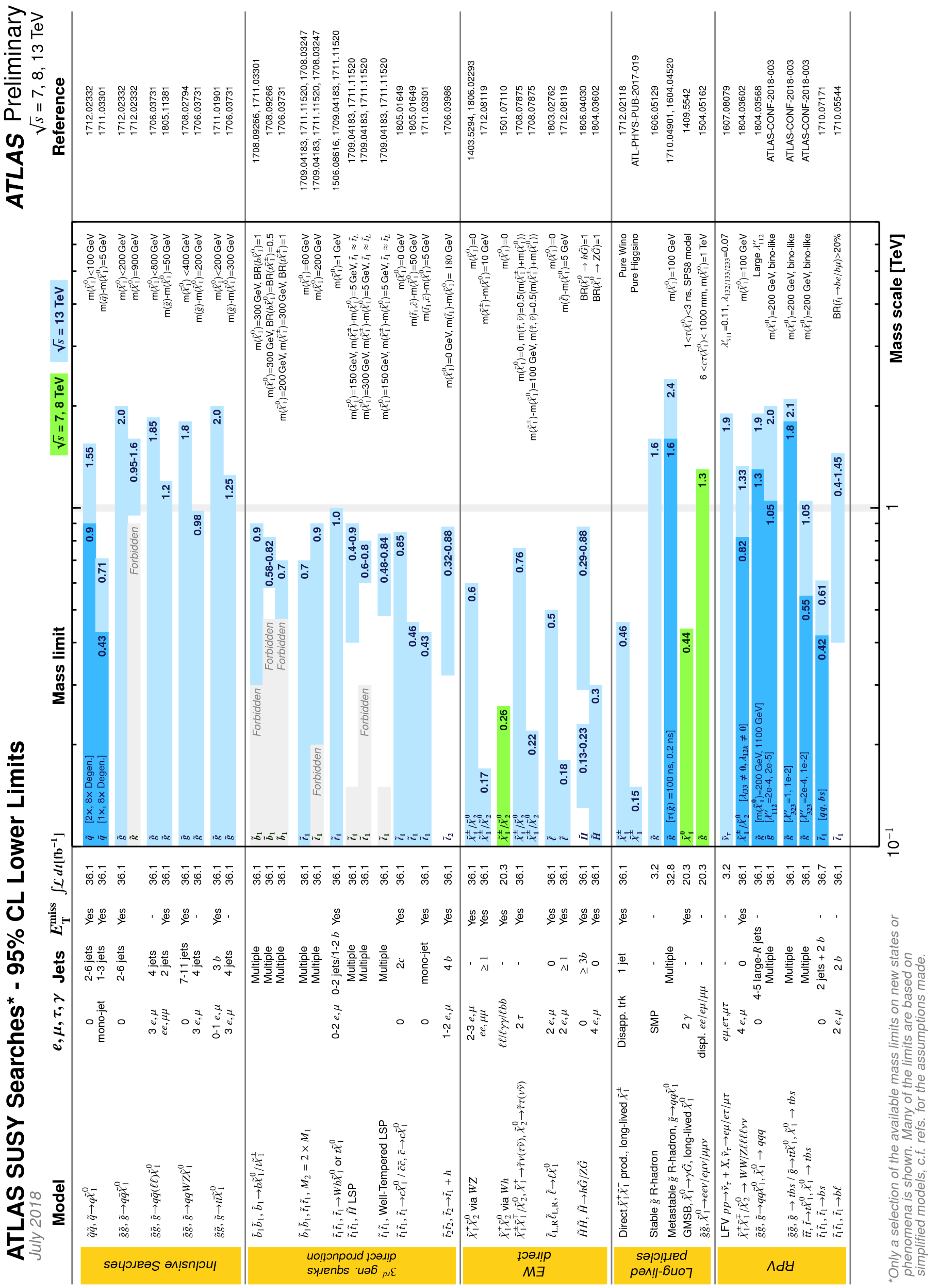

Figure 20: Summary of mass limits produced by the ATLAS experiment for different SUSY models [15].

Figure 21: Summary of mass limits produced by the CMS experiment for different SUSY models [16].

[10] Paul Jackson, Christopher Rogan, and Marco Santoni. Sparticles in motion: Analyzing compressed SUSY scenarios with a new method of event reconstruction. Phys. Rev. D, 95:035031, Feb 2017. doi:10.1103/PhysRevD.95.035031.

[11] P. Jackson and C. Rogan, Recursive Jigsaw Reconstruction: HEP event analysis in the presence of kinematic and combinatoric ambiguities, Phys. Rev. D 96 (2017) 112007, arXiv: 1705.10733 [hep-ph].

[12] The ATLAS collaboration, J. High Energ. Phys. (2018) 2018: 107. https://doi.org/10.1007/JHEP06(2018)107

[13] The ATLAS collaboration, ATLAS-CONF-2018-041, URL:https://cds.cern.ch/record/2632347

[14] The CMS collaboration, J. High Energ. Phys. (2019) 2019: 154. https://doi.org/10.1007/JHEP01(2019)154

[15] https://twiki.cern.ch/twiki/bin/view/AtlasPublic/SupersymmetryPublicResults

[16] https://twiki.cern.ch/twiki/bin/view/CMSPublic/PhysicsResultsSUS

[17] The CMS Collaboration, Phys. Rev. D, 99, 012010, 10.1103/PhysRevD 99.012010

[18] R. H. Dalitz, "Decay of tau mesons of known charge", Phys. Rev. 94 (1954) 1046-1051, doi:10.1103/PhysRev.94.1046.

[19] R. Barbieri and G. F. Giudice, Upper bounds on supersymmetric particle masses, Nucl. Phys. B 306 (1988) 63.

[20] B. de Carlos and J. A. Casas, One loop analysis of the electroweak breaking in supersymmetric models and the fine tuning problem, Phys. Lett. B 309 (1993) 320, arXiv: 9303291.

[21] K. Inoue, A. Kakuto, H. Komatsu and S. Takeshita, Aspects of grand unified models with softly broken supersymmetry, Prog. Theor. Phys. 68 (1982) 927, [Erratum: Prog. Theor. Phys. 70, 330 (1983)].

[22] J. R. Ellis and S. Rudaz, Search for supersymmetry in toponium decays, Phys. Lett. B 128 (1983) 248.

[23] The ATLAS collaboration, J. High Energ. Phys. (2018) 2018: 50. https://doi.org/10.1007/JHEP09(2018)050

[24] The ATLAS Collaboration, Optimisation of the ATLAS b-tagging performance for the 2016 LHC Run, ATL-PHYS-PUB-2016-012, 2016, url: https://cds.cern.ch/record/2160731

[25] The ATLAS Collaboration, Commissioning of the ATLAS b-tagging algorithms using $t\bar{t}$ events in early Run 2 data, ATL-PHYS-PUB-2015-039, 2015, url: https://cds.cern.ch/record/2047871.

[26] The CMS Collaboration, Phys. Lett. B 790 (2019) 005, https://doi.org/10.1016/j.physletb.2019.01.005

[27] The ATLAS collaboration, Eur. Phys. J. C (2018) 78: 995. https://doi.org/10.1140/epjc/s10052-018-6423-7

[28] The ATLAS collaboration, Phys. Rev. D 98, 092012, 10.1103/PhysRevD.98.092012

[29] The ATLAS Collaboration, Search for electroweak production of supersymmetric particles in final states with two or three leptons at $\sqrt{s} = 13$ TeV with the ATLAS detector, (2018), arXiv: 1803.02762 [hep-ex]